

Non-Adiabatic Contributions to the Free Energy from the Electron-Phonon Interaction for Na, K, Al, and Pb

N. Bock*

Theoretical Division, Los Alamos National Laboratory, Los Alamos, New Mexico 87545

D. Coffey

Dept. of Physics, Buffalo State College, Buffalo, New York 14222

Duane C. Wallace

Theoretical Division, Los Alamos National Laboratory, Los Alamos, New Mexico 87545

(Dated: October 6, 2018)

We calculate the non-adiabatic contributions to the free energy of metals due to the electron-phonon interaction at intermediate temperatures, $0 \leq k_B T < \epsilon_F$ for four different nearly free electron metals, Na, K, Al, and Pb. We calculate its value for $T = 0$ which has not been calculated before and we study its low-temperature behavior.

LA-UR-04-8709

PACS numbers: 64.70.Dv, 05.70.Ce, 63.70.+h, 64.10.+h

I. INTRODUCTION

For many practical applications one needs accurate values of thermodynamic properties of solids and liquids both at low pressures, where direct measurements are available, and in regions of temperature and pressure where data are absent. This requires a model Hamiltonian for the system which gives accurate results for the Helmholtz free energy. For a metal crystal the free energy consists of three contributions,

$$\begin{aligned} F &= \Phi_0(V) + F_E(V, T) + F_I(V, T) \\ &= \Phi_0(V) + F_{el}(V, T) + F_{ep}(V, T) \\ &\quad + F_{ph}(V, T) + F_{anh}(V, T). \end{aligned} \quad (1)$$

$\Phi_0(V)$, the static lattice potential, represents the total energy when the ions are located at lattice sites and the electrons are in their ground state. $F_I(V, T)$ is the free energy from ion vibrations, and $F_E(V, T)$ is the free energy associated with thermal excitation of electrons from their ground state. $F_I(V, T)$ is the dominant temperature contribution. It consists of the quasi-harmonic phonon contribution, $F_{ph}(V, T)$, plus the small anharmonic term $F_{anh}(V, T)$ which expresses phonon-phonon interactions. $F_E(V, T)$ consists of $F_{el}(V, T)$ representing the thermal excitation of independent electrons, plus $F_{ep}(V, T)$, the contribution from interactions between electronic excitations and phonons.

In this paper we determine the magnitude and temperature dependence of the non-adiabatic contributions to the free energy from the electron-phonon interaction for different metals and compare with previous treatments.

Our calculations are done for a constant density ρ to eliminate concern for the density dependence of phonon frequencies and electron-phonon interaction matrix elements. The density is that at the temperature T_ρ ,

where the phonon frequencies are measured. The melting temperature at this density is higher than the customary zero-pressure melting temperature. Our calculations cover the range from $T = 0$ to above T_m .

The paper is organized as follows: In section II we will introduce the expressions used for the electron-phonon part of the free energy. In section III our results are presented with a more detailed discussion of the numerical methods used.

II. ELECTRON-PHONON FREE ENERGY

A. Analytic Form of the Free Energy

Let us briefly discuss the physical origin of the contributions to F_{ep} , and show in the process that our formulation is free of double-counting errors. In electronic structure theory we calculate the electronic ground state energy with static nuclei, as a function of the nuclear positions, $\{\vec{r}_K\} = \vec{r}_{K=1, \dots, N}$. This energy is the ground state adiabatic potential $\Phi(\{\vec{r}_K\})$, which is resolved into $\Phi_0 + \Phi_{ph} + \Phi_{anh}$, and which together with the nuclear kinetic energy gives the free energy contribution $\Phi_0 + F_{ph} + F_{anh}$ in eq. (1). We next do the same calculation for the excited electronic states, labeled $n = 1, 2, \dots$ of the energy $E_n(\{\vec{r}_K\})$ with static nuclei. Here only the *excitation* energies $E_n - \Phi$ are considered since Φ is already included in the nuclear motion contributions. Excited electronic states with nuclei at the crystal lattice sites are calculated in electronic structure theory, and their energy levels are expressed in the electronic density of states, which provides the free energy contribution F_{el} in eq. (1). Next the thermally averaged vibrational contributions to the excited energies $E_n - \Phi$ are calculated, and these contributions yield the adiabatic part F^{ad} of the electron-phonon free energy, eq.

(3). Finally the non-adiabatic correction to all the electronic energy levels, ground and excited states alike, is calculated by allowing the nuclear motion to mix the electronic states. This produces the terms $F_1^{na} + F_2^{na}$, eqs. (4) and (5). The non-adiabatic part can formally be attributed to the terms in the trace of the partition function in which the nuclear kinetic energy operator operates on the electronic wavefunctions. A detailed discussion of the resolution of the crystal Hamiltonian, and the corresponding free energy contributions may be found in Wallace¹ Secs. 4 and 18 and pp. 91 – 94.

While this theory is valid for metals in general, an approximation is available from which we can calculate F_{ep} from previously calibrated models for the nearly-free electron metals. This is pseudopotential perturbation theory, which starts from free electrons in zeroth order, and treats the screened electron-ion interaction (the

pseudopotential) as a perturbation. Electronic band-structure effects then arise in standard perturbation theory. The electron-phonon theory becomes a double perturbation expansion, in the pseudopotential and in the displacement of nuclei from equilibrium. But the displacement expansion converts to a pseudopotential expansion, and the leading contributions to F_{ep} are all of second order in the pseudopotential. The derivation may be found in¹ (Sec. 18).

The electron-phonon contribution is written as a sum over the three terms mentioned in the previous paragraph. They are

$$F_{ep} = F^{ad} + F_1^{na} + F_2^{na}, \quad (2)$$

where the single contributions are given by

$$\frac{F^{ad}}{N} = \sum_{\vec{p}\vec{k}\vec{Q}\lambda} \frac{\hbar^2}{N^2 M} \frac{n_{\vec{k}\lambda} + \frac{1}{2}}{\hbar\omega_{\vec{k}\lambda}} (f_{\vec{p}} - g_{\vec{p}}) \left\{ \frac{[(\vec{k} + \vec{Q}) \cdot \hat{\eta}_{\vec{k}\lambda}]^2 [U(\vec{k} + \vec{Q})]^2}{\epsilon_{\vec{p}} - \epsilon_{\vec{p} + \vec{k} + \vec{Q}}} - \frac{[\vec{Q} \cdot \hat{\eta}_{\vec{k}\lambda}]^2 [U(\vec{Q})]^2}{\epsilon_{\vec{p}} - \epsilon_{\vec{p} + \vec{Q}}} \right\} \quad (3)$$

$$\frac{F_1^{na}}{N} = \sum_{\vec{p}\vec{k}\vec{Q}\lambda} \frac{\hbar^2}{N^2 M} \hbar\omega_{\vec{k}\lambda} \left(n_{\vec{k}\lambda} + \frac{1}{2} \right) \frac{f_{\vec{p}}}{\epsilon_{\vec{p}} - \epsilon_{\vec{p} + \vec{k} + \vec{Q}}} \frac{[(\vec{k} + \vec{Q}) \cdot \hat{\eta}_{\vec{k}\lambda}]^2 [U(\vec{k} + \vec{Q})]^2}{[\epsilon_{\vec{p}} - \epsilon_{\vec{p} + \vec{k} + \vec{Q}}]^2 - [\hbar\omega_{\vec{k}\lambda}]^2} \quad (4)$$

$$\frac{F_2^{na}}{N} = \sum_{\vec{p}\vec{k}\vec{Q}\lambda} \frac{\hbar^2}{2N^2 M} f_{\vec{p}} (1 - f_{\vec{p} + \vec{k} + \vec{Q}}) \frac{[(\vec{k} + \vec{Q}) \cdot \hat{\eta}_{\vec{k}\lambda}]^2 [U(\vec{k} + \vec{Q})]^2}{[\epsilon_{\vec{p}} - \epsilon_{\vec{p} + \vec{k} + \vec{Q}}]^2 - [\hbar\omega_{\vec{k}\lambda}]^2}. \quad (5)$$

Here and in the following we will calculate and quote our results as per atom. $f_{\vec{p}}$ is the Fermi-Dirac distribution function at finite temperature and $g_{\vec{p}}$ is the same at $T = 0$. $n_{\vec{k}\lambda}$ is the Bose-Einstein distribution function at finite temperature and $\hat{\eta}_{\vec{k}\lambda}$ is the polarization vector of the phonon branch λ for wave vector \vec{k} which is inside the Brillouin zone. \vec{Q} is a reciprocal lattice vector and $\omega_{\vec{k}\lambda}$ is the frequency of a phonon mode. $U(\vec{k} + \vec{Q})$ is the Fourier transform of the pseudopotential for momentum transfer $\vec{k} + \vec{Q}$. In our calculations we use two models for the pseudopotential, the Harrison and the Ashcroft models, which are screened by exchange and electron-electron interactions (detailed forms are given in Wallace², pp. 312). The pseudopotential parameters are listed in Table II. $\epsilon_{\vec{p}}$ is the electron energy measured relative to the Fermi energy.

In the above formulas, every term is of second order in $U(q)$. The appearance of free electron energies in the denominators results from the use of perturbation theory. The pseudopotential modification of the electron wavefunctions gives rise to the last term in braces in eq. (3). An alternate derivation, by means of Matsubara frequen-

cies, is outlined in the appendix.

This is the form of the electron-phonon contribution to the free energy originally calculated by Eliashberg³ who studied the electron-phonon interaction in the superconducting state. It is known that the non-adiabatic contribution dominates the adiabatic one at low temperature⁴ and we will focus on $F_{1,2}^{na}$ in this paper. F^{ad} will be examined in a future publication.

B. Analytic temperature dependences

From eqs. (4) and (5) we estimate the low- T dependence of the two non-adiabatic contributions with the leading order terms of a Sommerfeld expansion⁵ (pp. 45). This is certainly accurate for nearly free electron metals which have smooth density of states around the Fermi surface, but is less certain for transition metals and actinides because their electronic density of states tends to fluctuate strongly around the Fermi surface which makes power series expansions around ϵ_F less accurate.

1. F_1^{na}

In order to analyze the first non-adiabatic contribution we rewrite the Fermi-Dirac factor as follows:

$$f_{\vec{p}} = g_{\vec{p}} + (f_{\vec{p}} - g_{\vec{p}}). \quad (6)$$

At high temperatures we can expand the other temperature dependent factor

$$\hbar\omega \left(n_{\vec{k}} + \frac{1}{2} \right) = \hbar\omega \left\{ \frac{1}{\beta\hbar\omega} + \frac{\beta\hbar\omega}{12} + \frac{(\beta\hbar\omega)^3}{720} + \dots \right\} \quad (7)$$

in powers of T and get a linear T dependence in leading order. At low temperature, the factor eq. (7) will go over to a constant and we find that the temperature dependence of the ground state part of F_1^{na} given by the first term in eq. (6) will be given by

$$F_1^{na} = \begin{cases} \text{const. at } T = 0 \\ kT \text{ at high } T \end{cases} \quad (8)$$

The contribution from the term in parentheses in eq. (6) is restricted in phase space to a small volume around the Fermi surface, whereas the ground state contribution is restricted only to $p < p_F$. Since the $(f_{\vec{p}} - g_{\vec{p}})$ contribution has much less phase space than the $g_{\vec{p}}$ contribution, the ground state contribution will dominate at all temperatures and we will not see any additional temperature dependence beyond eq. (8).

Considering the factor $\hbar\omega / (\epsilon_{\vec{p}} - \epsilon_{\vec{p}'})$ in F_1^{na} we expect this contribution to be of order $\hbar\langle\omega\rangle/\epsilon_F$ smaller than F_2^{na} and we will be able to neglect it. We calculated F_1^{na} for Na to verify these estimates and present it in section III.

2. F_2^{na}

Taking a closer look at the integrand of the second non-adiabatic contribution we notice that all factors but one are positive for all points in the integration region. Only the energy difference in the denominator can have different signs depending on the momenta \vec{p} and $\vec{p}' = \vec{p} + \vec{k} + \vec{Q}$. We estimate its sign by dividing the integration phase space into two regions

$$|\Delta\epsilon| = \left| \epsilon_{\vec{p}} - \epsilon_{\vec{p}'} \right| \begin{cases} < \hbar\omega & \text{(Region 1)} \\ > \hbar\omega & \text{(Region 2)} \end{cases} \quad (9)$$

At zero temperature due to the Fermi-Dirac factor, $f_{\vec{p}}(1 - f_{\vec{p}'})$, the width of the phase space for Region 1 is twice the phonon energy, $2\hbar\omega$, in energy around the Fermi surface and very small compared to Region 2 which

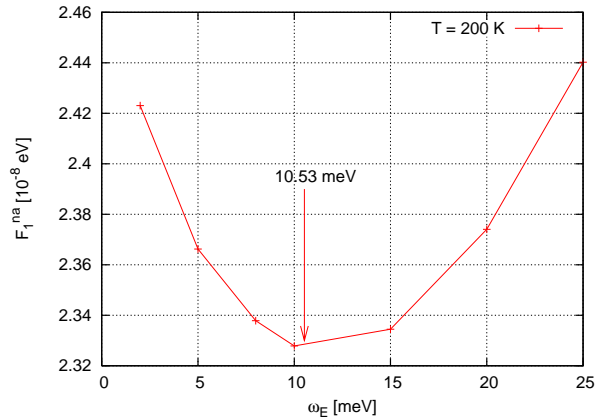


FIG. 1: ω_E -dependence of F_1^{na} for Na at $T = 200$ K.

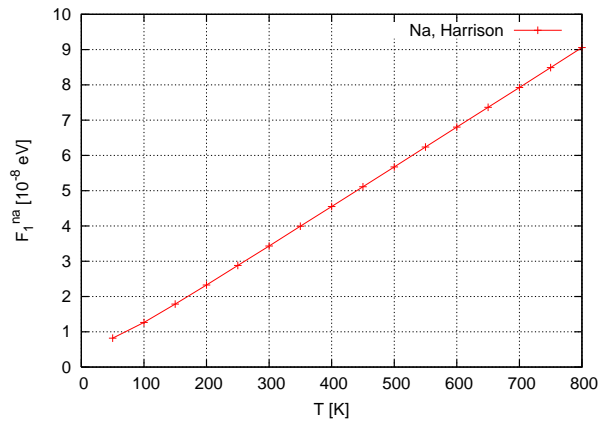


FIG. 2: F_1^{na} for Na.

extends everywhere outside Region 1. $F_2^{na}(T = 0)$ will therefore be positive. Increasing temperature will widen the phase space for Region 1 because of the softening of the Fermi surface and will increase its negative contribution to the total but will leave the contribution from Region 2 mostly unaffected. The overall effect will be to reduce the magnitude of F_2^{na} , the more so with increasing temperature but we expect F_2^{na} to remain positive.

From a Sommerfeld expansion of the Fermi-Dirac factor for small temperatures we estimate the low-temperature dependence of F_2^{na} to be given by

$$F_2^{na} = C_2 + A_2 T^2 + \dots \quad (10)$$

Previous work on the electron-phonon contribution to the free energy focused on calculating the specific heat and missed the factor C_2 which we will calculate in section III. An extensive survey of the theoretical calculations is given by Grimvall⁶ (Tables III-VI). We will also calculate the factor A_2 and compare with experiment and previous estimates for different materials.

As has been shown by previous authors, the low temperature specific heat of normal metals has a $T^3 \ln T$ contribution which comes from electron-electron interaction,

both those induced by phonons and those due to the Coulomb interaction. Coffey and Pethick⁷ and Danino and Overhauser⁸ for instance derived this contribution for a Debye model. We are using an Einstein model in our calculations of the non-adiabatic parts and can not pick up the $T^3 \ln T$ term since it depends on the existence of acoustic phonon modes. It is known however that this contribution is small compared to the others and we will not calculate it.

III. RESULTS

A. Einstein Approximation

In this section we want to study the two non-adiabatic contributions using an Einstein model. We will try to answer two main questions: Will we get the correct temperature dependence from such a simplified model? How accurate will our results be?

The details of the phonon model enter the single contributions through the factor

$$\left[(\vec{k} + \vec{Q}) \cdot \hat{\eta}_{\vec{k}\lambda} \right]^2 \quad (11)$$

in the integrands and through their explicit dependence on the phonon frequencies, $\omega_{\vec{k}\lambda}$. The former contains details of the phonon spectrum in terms of the polarization vectors of the phonon branches and turns out to have a fairly weak effect on the integral, whereas the effect of the latter can be very strong for acoustic phonon branches. When \vec{k} goes to zero at the zone center¹⁶ the phonon frequencies of acoustic branches vanish. If the integrand plus volume factors of k^2 is well-behaved and finite for $\omega_{\vec{k}\lambda} \rightarrow 0$ we can expect to be able to approximate the integral using a suitably chosen Einstein mode. If the integrand plus volume factors diverges for vanishing $\omega_{\vec{k}\lambda}$ the details of the phonon spectrum will be important and we can not expect to be able to approximate the full phonon spectrum with a single frequency. There might be a situation of course in which a single phonon frequency will result in the correct temperature dependence, but without calculating the integral using a realistic phonon dispersion we have no way of knowing what that single frequency should be.

Both non-adiabatic contributions, $F_{1,2}^{na}$, have the factor

$$\frac{1}{\left[\epsilon_{\vec{p}} - \epsilon_{\vec{p}+\vec{k}+\vec{Q}} \right]^2 - [\hbar\omega_{\vec{k}\lambda}]^2}, \quad (12)$$

in common. At the zone center this turns into

$$\frac{1}{\left[\epsilon_{\vec{p}} - \epsilon_{\vec{p}+\vec{k}+\vec{Q}} \right]^2} \quad (13)$$

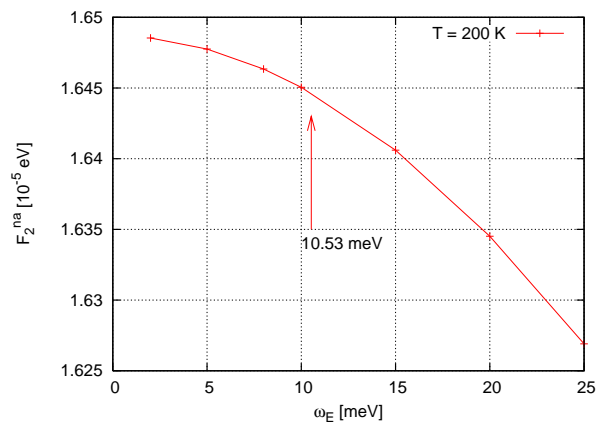


FIG. 3: ω_E -dependence of F_2^{na} for Na at $T = 200$ K.

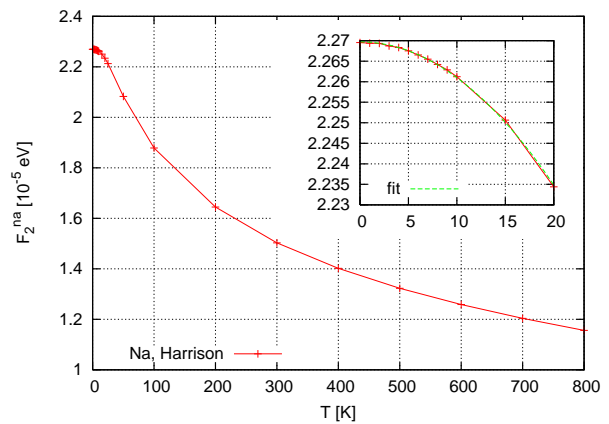


FIG. 4: F_2^{na} for Na. The inset shows the low temperature region.

which is well behaved¹⁷. The additional factor

$$\lim_{\omega_{\vec{k}\lambda} \rightarrow 0} \hbar\omega_{\vec{k}\lambda} \left(n_{\vec{k}\lambda} + \frac{1}{2} \right) = k_B T \quad (14)$$

in F_1^{na} is also well behaved at the Γ point. We conclude that a single phonon frequency will reproduce $F_{1,2}^{na}$ with the correct temperature dependence. We also expect it to be accurate and we will quantify this last statement later in this paper.

Figs. 1 and 3 show the non-adiabatic contributions for an Einstein model at $T = 200$ K. Our a priori estimate for the Einstein frequency is $\omega_E = \langle \omega \rangle$, where $\langle \omega \rangle$ is the average over the Brillouin zone. For reference we included our estimates for the average phonon frequency in the graphs and in Table I. As expected, the frequency dependence is very weak and we can neglect it.

B. Numerical Techniques

The two sums over the electron and phonon momenta, $\sum_{\vec{p}}$ and $\sum_{\vec{k}\vec{Q}}$, are over all of reciprocal space. Assuming

a large sample size we therefore have the option to convert one or both of these sums into integrals, using the well known relationship

$$\sum_{\vec{p}} = \frac{NV_A}{(2\pi)^3} \int d^3p, \quad (15)$$

where N is the number of ions in the sample, and V_A the volume per ion. In general, due to the completeness of the phonon eigenvectors in 3 dimensional space,

$$\sum_{\lambda} [(\vec{k} + \vec{Q}) \cdot \hat{\eta}_{\vec{k}\lambda}]^2 = |\vec{k} + \vec{Q}|^2. \quad (16)$$

In an Einstein model the sum over phonon branches can be performed outside the integral since the only factors that depend on the branch index, λ , are contained in eq. (16). This means that the integrand does not depend on the crystal structure. If we combine the double sum $\sum_{\vec{k}\vec{Q}}$ with $\sum_{\vec{p}}$ where $\vec{p}' = \vec{p} + \vec{k} + \vec{Q}$ we can replace both sums, $\sum_{\vec{p}\vec{p}'}$, in the two non-adiabatic contributions with integrals without loss of generality. Eqs. (4) and (5) can then be written as

$$\frac{F_1^{na}}{N} = \frac{V_A^2}{(2\pi)^6} \mathcal{P} \int d\vec{p} \int d\vec{p}' \frac{\hbar^2}{M} \hbar\omega_E \left(n_E + \frac{1}{2} \right) \frac{f_{\vec{p}}}{\epsilon_{\vec{p}} - \epsilon_{\vec{p}'}} \frac{|\vec{p}' - \vec{p}|^2 [U(\vec{p}' - \vec{p})]^2}{[\epsilon_{\vec{p}} - \epsilon_{\vec{p}'}]^2 - [\hbar\omega_E]^2} \quad (17)$$

$$\frac{F_2^{na}}{N} = \frac{V_A^2}{(2\pi)^6} \mathcal{P} \int d\vec{p} \int d\vec{p}' \frac{\hbar^2}{2M} f_{\vec{p}} (1 - f_{\vec{p}'}) \frac{|\vec{p}' - \vec{p}|^2 [U(\vec{p}' - \vec{p})]^2}{[\epsilon_{\vec{p}} - \epsilon_{\vec{p}'}]^2 - [\hbar\omega_E]^2}, \quad (18)$$

where \mathcal{P} stands for the principal part. We would like to mention that neither one of the two non-adiabatic contributions has any obvious upper limits for the integration on \vec{p}' and we need to make sure that we understand the convergence behavior of their integrands for large $|\vec{p}'|$. The pseudopotential, $U(\vec{q})$, converges as q^{-2} for large q and we conclude that the second non-adiabatic contribution, F_2^{na} , converges as $(p')^{-4}$. Due to the additional factor of $1/(\epsilon_p - \epsilon_{p'})$ in F_1^{na} , the first non-adiabatic contribution converges as $(p')^{-6}$. We can therefore expect good convergence behavior for the two non-adiabatic contributions in terms of the integration over $\vec{p}' = \vec{p} + \vec{k} + \vec{Q}$. Fig. 5 shows this nicely. p_{\max} is the upper integration limit of p' .

The 6-dimensional integration of eqs. (17) and (18) was done using the VEGAS method^{9,10}. We took special care to ensure convergence around the divergent poles of the integrands when calculating the principal part. This was done by first reducing the poles from second to first order and then removing the divergence by subtracting a suitably chosen function from the integrand and integrating its pole by hand. This effectively smoothed the integrand sufficiently so that our VEGAS calculation converged much more rapidly. It also improved the reliability of the VEGAS error estimate and therefore the accuracy of our calculation. Since we are using spherical coordinates, this procedure has the advantage that we can very efficiently limit the integration region around the Fermi surface by using appropriate integration lim-

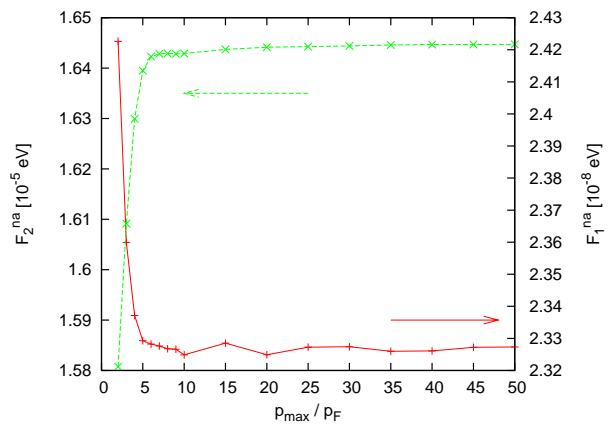


FIG. 5: Convergence of F_1^{na} and F_2^{na} for Na at $T = 200$ K.

its. It is also simpler to implement than a tetrahedron method in which the Brillouin zone is divided into tetrahedra which are then summed up.

C. Non-Adiabatic Contribution to F_{ep} for different materials

We calculated F_1^{na} for Na and F_2^{na} for Na, K, Al, and Pb. Table I shows the material specific constants used in our calculations.

Figs. 2 and 4 show our results for Na using a single

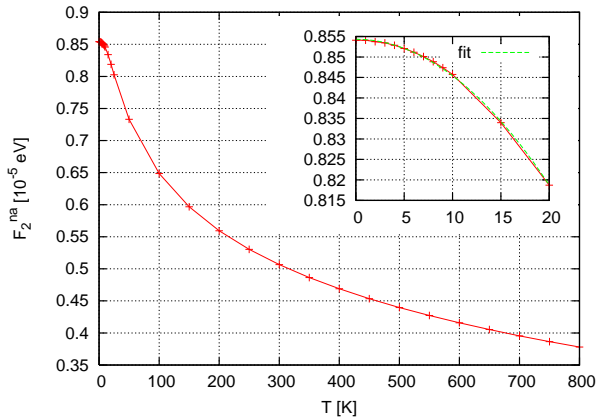
FIG. 6: F_2^{na} for K, Harrison model.

TABLE I: Material constants

	Na	K	Al	Pb
structure	bcc	bcc	fcc	fcc
T_ρ [K]	90	9	80	80
ρ [g cm $^{-3}$]	1.005	0.904	2.731	11.55
$\langle \hbar\omega \rangle$ [meV]	10.53	6.42	25.79	5.90
a [Å]	4.23	5.24	4.05	4.95
p_F [Å $^{-1}$]	0.92	0.74	1.75	1.57
ϵ_F [eV]	3.24	2.11	11.66	9.45
T_{melt} [K]	407	368	1234	722

phonon mode at $\hbar\omega_E = 10.53$ meV for $F_{1,2}^{na}$. F_1^{na} exhibits linear temperature dependence for higher temperatures and even at temperatures as low as 50 K we hardly see deviations from linear behavior. This confirms our previous estimate of this contribution's temperature dependence based on a phase space argument. In section II B we had argued that when we rewrite the Fermi-Dirac distribution factor in eq. (17) as eq. (6) we expect the $g_{\vec{p}}$ -factor to be dominant due to its much larger phase space. Since $g_{\vec{p}}$ is not temperature dependent, the only temperature dependent factor is the phonon distribution which is linear at high temperatures. As we had argued in the same section also, the magnitude of F_1^{na} is much smaller than the magnitude of F_2^{na} . Based on this magnitude differ-

TABLE II: The pseudopotential parameters. Parameters for the Harrison model are $\hat{\rho}$ and $\hat{\beta}$, while the single parameter for the Ashcroft model is $\bar{\rho}$.

	Na	K	Al	Pb
Reference	² (p. 406)	² (p. 406)	² (p. 415)	¹¹ (p. 502)
Z	1	1	3	4
ξ	1.81	1.77	1.90	1.81
$\hat{\rho}$ [a_B]	0.50	0.69	0.24	—
$\hat{\beta}$ [Ry a_B^3]	37	66	47.5	—
$\bar{\rho}$ [a_B]	—	—	1.117	1.12

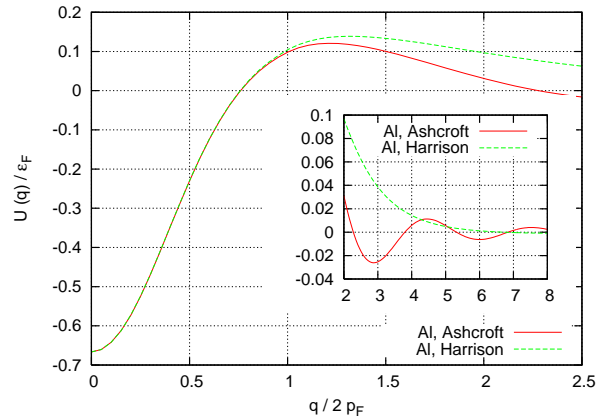


FIG. 7: Harrison and Ashcroft pseudopotential models for Al. The parameters are given in Table II.

ence we will neglect F_1^{na} from this point onward.

Fig. 4 shows F_2^{na} and as expected this contribution is positive all throughout the temperature regime shown. Starting from $T = 0$ the curve has negative curvature but quickly switches to positive curvature and never crosses zero even at high temperatures. From the inset in Fig. 4 we get the values of C_2 and A_2 listed in Table III.

Fig. 6 shows our result for F_2^{na} for K. The magnitude of the F_2^{na} contribution is smaller by about a factor of 3 compared to Na. The difference is presumably largely due to the difference in ϵ_F which affects the size of the pseudopotential $U(q)$. Since the ratio of Fermi energies is about 3/2 and the pseudopotential enters the free energy squared, we get about a factor of 2 difference between the two materials just based on this term.

The pseudopotentials for Al are shown in Fig. 7. Between zero and $q/(2p_F) \approx 1$ the two models are identical. Between $1 \lesssim q/(2p_F) \lesssim 4$ the Harrison model is larger than the Ashcroft model and for $q/(2p_F) \gtrsim 4$ both models slowly approach zero. Fig. 8 shows our results for Al which we calculated for these two pseudopotential models. F_2^{na} using an Ashcroft pseudopotential model is shifted by about 0.05 meV to lower energies compared to the Harrison model. The qualitative temperature dependence is not affected. The difference between the two models in terms of their convergence to zero for large q therefore does not appear to be relevant in affecting the temperature dependence of F_2^{na} . The difference in magnitude for intermediate q does enter the overall magnitude of F_2^{na} and makes a difference of about 20 - 30%. The inset Fig. 8 shows a fit using eq. 10, and the results for C_2 and A_2 are listed in Table III.

Fig. 9 shows our results for Pb. In Fig. 10 we show the entropy calculated from the free energy and compare our result with earlier results by Grimvall¹², Fig. 5.19. Our results are scaled with an Einstein temperature of $\langle \hbar\omega \rangle = 5.9$ meV = 68.5 K. We find very good agreement with Grimvall's results. Grimvall calculated the total entropy, i.e. $S_{Grimvall} = S^{ad} + S_1^{na} + S_2^{na}$ for Pb up to $T = 1.4 T_E$. Up to this temperature, our purely

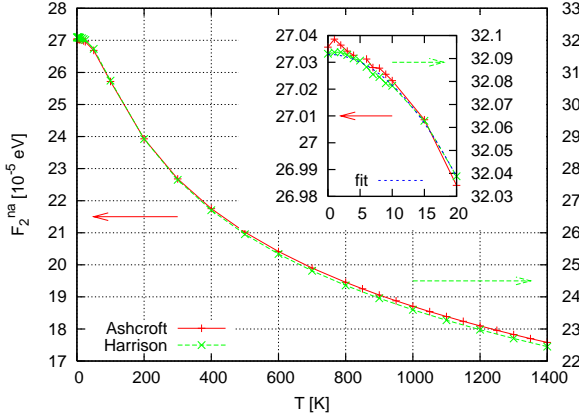


FIG. 8: F_2^{na} for Al for different pseudopotential models.

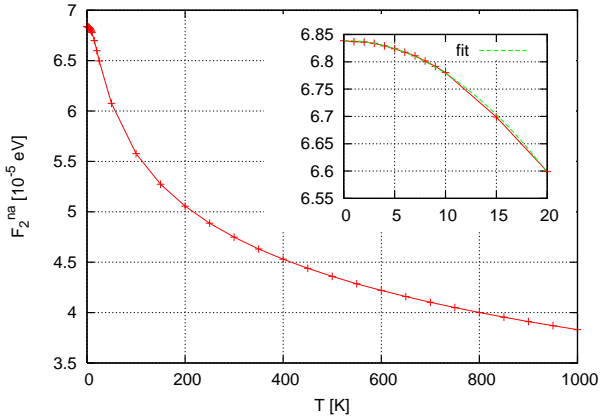


FIG. 9: F_2^{na} for Pb, Ashcroft pseudopotential model.

non-adiabatic entropy, S_2^{na} , agrees very nicely with his results¹⁸. The adiabatic contribution remains small compared to the non-adiabatic up to much higher temperatures. We shall address this in a future publication.

IV. CONCLUSIONS

A thorough analysis of the first non-adiabatic term, F_1^{na} , reveals a ground state contribution, $\propto g_{\bar{p}}$, and a contribution due to excited electronic states, $\propto (f_{\bar{p}} - g_{\bar{p}})$, cf. eq. (6). We find that the ground state term, since its temperature dependence is determined by the phonon factor alone, leads to a T -dependence of F_1^{na} as given in eq. (8). Electronic excitations above the ground state, the $(f_{\bar{p}} - g_{\bar{p}})$ term, will lead to a temperature dependence which is determined by the leading terms in a Sommerfeld expansion and give a T^2 -dependence at low temperatures for F_1^{na} . Using a phase space argument we found that the ground state term will dominate the temperature dependence and essentially determine it. The contribution from the excited electronic states to the temperature dependence will be much smaller than the ground state contribution and not visible in our calculations. We also

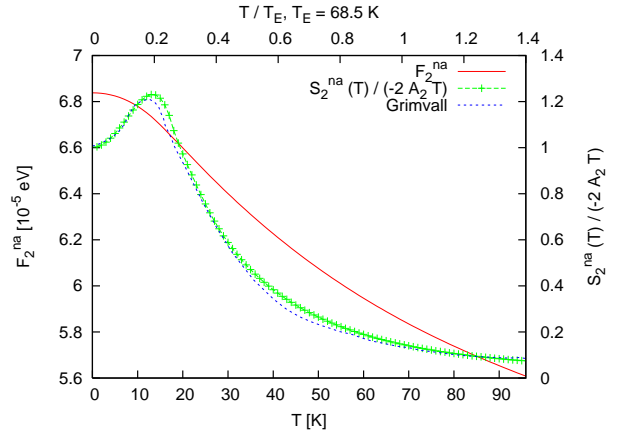


FIG. 10: F_2^{na} and $S_2^{na}(T)/(-2A_2T)$, where A_2 was defined in eq. (10), compared with earlier results by Grimvall on Pb. F_2^{na} is plotted with axes on the left and bottom, S_2^{na} and Grimvall's results are plotted with axes on the right and top.

TABLE III: $F_2^{na}(T=0)$ and curvatures at low- T (Units: C_2 [10^{-8} eV/atom], A_2 [10^{-5} eV/atom K^2])

	Na	K	Al	Pb
C_2 (Harrison)	2.270	0.8543	32.09	—
C_2 (Ashcroft)	—	—	27.04	6.839
(expt. ^a)	-0.10	-0.13	-0.19	-0.86
² (Table 27)	-0.14	-0.14	-0.30	—
A_2 (ppt ^b)	-0.10	-0.12	-0.24	-0.91
(Harrison)	-0.0878	-0.0889	-0.1316	—
(Ashcroft)	—	—	-0.1285	-0.6039

^a A_2 is calculated from experiment using low-temperature specific heat data. From eq. (10) we find $C_{ep} = -2A_2T$. At low T , $C_{expt} = \Gamma_{expt}T$ and $C_{th} = \Gamma_{bs}(1 + \lambda)T$. Our $C_{ep} = \lambda\Gamma_{bs}T$ and we find $A_2 = -\frac{1}{2}(\Gamma_{expt} - \Gamma_{bs})$. Γ_{expt} taken from Kittel¹³, Table on p. 157. The analysis was done by Allen¹⁴, Table I and eq. (6).

^b A_2 is calculated from pseudopotential perturbation theory, and given by $A_2 = -\frac{1}{2}\Gamma_{bs}\lambda$. λ is taken from the data collection of Grimvall⁶, Tables III, IV, and V.

expect the magnitude of F_1^{na} to be $\propto (\langle \hbar\omega \rangle / \epsilon_F) F_2^{na}$ and hence negligible compared to F_2^{na} . Our numerical results confirm our suspicions, cf. Fig. 2. The calculated temperature dependence is linear, i.e. the ground state term dominates the temperature dependence of F_1^{na} . The absolute magnitude of F_1^{na} is by about three orders of magnitude smaller than what we find for F_2^{na} and we find that we can neglect this contribution.

The more complicated dependence of the Fermi-Dirac factor does not allow us to split $f_{\bar{p}}(1 - f_{\bar{p}'})$ into parts as in eq. (6), and the low-temperature dependence of F_2^{na} is determined by the leading terms in a Sommerfeld expansion. The T -dependence therefore is given by eq. (10). Studying the sign of the single factors in F_2^{na} we find that this contribution is positive for all temperatures. Starting from a non-zero constant at $T = 0$ the magnitude slowly approaches zero as the temperature in-

creases. Our numerical results confirm this analysis, cf. Fig. 4. The constant C_2 is the non-adiabatic correction to the adiabatic ground state energy¹, $\Phi_0(V)$. In general $C_2 \ll \Phi_0$ and is negligible. The curvature A_2 represents the leading electron-phonon correction to the low-temperature free energy and specific heat. The latter can be written as

$$C = \frac{\pi^2}{3} N_{bs} k_B^2 (1 + \lambda) T, \quad (19)$$

where the electronic density of states given by band-structure alone, N_{bs} , comes from \mathcal{H}_{el} and is corrected by the electron-phonon interaction with the factor λ . This factor is measurable in experiments and can get quite large for certain metals. In the case of lead for instance, $\lambda \approx 1.2$. We calculated the constant C_2 and the curvature A_2 for all four metals we studied and our results are listed in Table III. In addition to our results we also included results from experiment and from previous theoretical studies. Our results agree fairly well with the other numbers. It should be pointed out that while F_2^{na} is important for low temperatures, it is negligible at high- T . Comparing the entropy from the non-adiabatic contribution with the electronic contribution for instance, the ratio S_2^{na}/S_{el} while important at low temperatures, becomes negligible for $T/T_E \gtrsim 1$.

Our results in Table III indicate variations in the different theoretical calculations. But regardless of the details of the theoretical description, they show the ability of the theory to calculate the experimental results. Since we are working within the Einstein approximation, they also provide confirmation of our previous assumption that the Einstein model will give us the correct temperature dependence and accurate results.


APPENDIX A: TECHNICAL DETAILS REGARDING THE CALCULATION

We used a diagrammatic technique to calculate the electron-phonon contribution eq. (2). To leading order in the interaction however this approach is completely equivalent to a standard perturbation theory approach

taken by Wallace for instance² (Section 25). We used a linked cluster expansion, given by

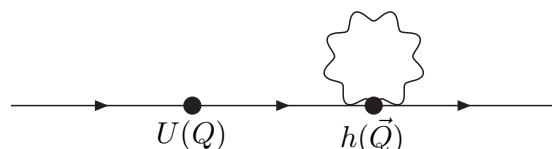
$$\Omega - \Omega_0 = \frac{1}{2\beta} \int_0^1 \frac{d\eta}{\eta} \sum_{\vec{k}\sigma} \sum_{ik_n} \Sigma^\eta(\vec{k}\sigma, ik_n) \mathcal{G}^\eta(\vec{k}\sigma, ik_n), \quad (A1)$$

where the self-energy and Green's function implicitly depend on the coupling constant¹⁵, η . Since we are using a plane wave basis and a free electron dispersion, we need to include the zeroth order term in \mathcal{H}_{ep} . The electron self energy, $\Sigma(\vec{k}, ik_n)$, includes diagrams of the form



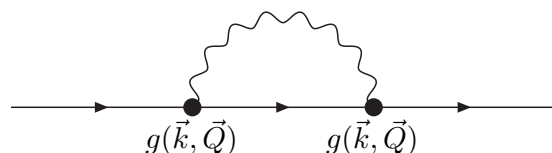
$$\text{---} \bullet \xrightarrow{U(Q)} \dots \xrightarrow{U(Q)} \bullet \text{---} \quad (A2)$$

in n^{th} order. We therefore do not consider these terms in \mathcal{H}_{ep} . We do need to correct our plane wave basis and include terms of the form



$$\text{---} \bullet \xrightarrow{U(Q)} \text{---} \text{---} \text{---} \text{---} \text{---} \text{---} \text{---} \text{---} \text{---} \text{---} \text{---} \bullet \xrightarrow{h(\vec{Q})} \text{---} \quad (A3)$$

This can be achieved in regular perturbation theory by correcting the wave function to first order and then calculating the diagonal matrix elements in first order. Eq. (25.17) of Wallace² corresponds to this kind of diagram. The first term in (25.21) therefore is given by



$$\text{---} \bullet \xrightarrow{g(\vec{k}, \vec{Q})} \text{---} \text{---} \text{---} \text{---} \text{---} \text{---} \text{---} \text{---} \text{---} \text{---} \bullet \xrightarrow{g(\vec{k}, \vec{Q})} \text{---} \quad (A4)$$

* Electronic address: nbock@lanl.gov

¹ D. C. Wallace, *Statistical Physics of Crystals and Liquids* (World Scientific Publishing Co. Pte. Ltd., 2002).

² D. C. Wallace, *Thermodynamics of Crystals* (John Wiley & Sons, Inc., 1972).

³ G. M. Eliashberg, *Sovet Phys. JETP* **11**, 696 (1960).

⁴ P. B. Allen, *Phys. Rev. B* **18**, 5217 (1978).

⁵ N. W. Ashcroft and N. D. Mermin, *Solid State Physics* (Holt, Rinehart and Winston, 1976).

⁶ G. Grimvall, *Physica Scripta* **14**, 63 (1976).

⁷ D. Coffey and C. J. Pethick, *Phys. Rev. B* **37**, 442 (1988).

⁸ M. Danino and A. W. Overhauser, *Phys. Rev. B* **26**, 1569 (1982).

⁹ G. P. Lepage, Cornell preprint CLNS p. 447 (1980).

¹⁰ W. H. Press, *Numerical Recipes in C: The Art of Scientific Computing* (Cambridge University Press, 1988).

¹¹ R. D. Parks, ed., *Superconductivity*, vol. 1 (Marcel Dekker, Inc., 1969).

¹² G. Grimvall, *The Electron-Phonon Interaction in Metals* (North-Holland Publishing Company, 1981).

¹³ C. Kittel, *Introduction to Solid State Physics* (Wiley, New York, 1996), 7th ed.

¹⁴ P. B. Allen, Phys. Rev. B **36**, 2920 (1987).

¹⁵ A. L. Fetter and J. D. Walecka, *Quantum Theory of Many-Particle Systems* (McGraw-Hill Inc, 1971).

¹⁶ We remind the reader that \vec{k} is restricted to the Brillouin zone.

¹⁷ We are working with a parabolic band and at Γ -points

with $\vec{Q} \neq 0$ the electronic energies $\epsilon_{\vec{p}} \neq \epsilon_{\vec{p}+\vec{Q}}$.

¹⁸ To remind the reader we would like to note that as pointed out previously, the first non-adiabatic contribution, F_1^{na} , and consequently its related entropy, S_1^{na} , is negligible compared to the other two contributions.